



OPEN A novel method for assessing postmortem interval using radon radioisotopic decay – an internal radon ‘time of death clock’

Behnam Ashrafkhani^{1✉}, Armin Tabesh¹, Fredrik Tamsen^{2,3}, Aaron A. Goodarzi⁴, Martin Tondel^{5,6}, Robert Ian Thompson¹ & Michael E. Wieser¹

Estimating the postmortem interval (PMI)—the time since death—remains a longstanding challenge in forensic and biological sciences due to the complex influence of environmental and physiological variables. Here, we present a novel computational framework that leverages the physical principles of radioactive decay to estimate PMI using the relative isotope abundances of radon progeny (^{210}Pb , ^{210}Bi , and ^{210}Po) in biological tissue. Our approach models the decay chain of inhaled ^{222}Rn and solves the associated system of differential equations to determine PMI based on isotope ratio dynamics. A key innovation is the use of paired measurements taken at two postmortem time points to capture the time-derivative of the decay curve, enhancing solution uniqueness, reducing dependence on prior exposure history, therefore minimizing error. Monte Carlo simulations were employed to assess model performance. If validated empirically, this approach lays the groundwork for a physics-based method for PMI estimation with potential applications in forensic science and radiation biology.

The amount of time that has elapsed since the death of an individual and discovery of their corpse is known as the postmortem interval (PMI) and, as it is typically very important for investigators to get an estimation of how long the person has been dead, is a challenging problem in forensic science^{1–3}. Indeed, the earliest documented study of PMI dates to the 13th century, with controlled scientific studies commencing in the 19th century⁴. Since then, a large number of methods have been explored, with an exponential increase in publications since the 1970s. Resulting PMI methods have been largely based on physical, biological, and biochemical indicators⁵. However, all PMI tools we have are subject to varying degrees of uncertainty that make it difficult to determine PMI with accuracy (*i.e.* PMI estimate reflects the actual time of death) and/or precision (*i.e.* PMI estimates are consistent between corpses with same time of death)^{5,6}. Current information used to estimate PMI can be broadly divided into three groups based on the source information: circumstantial evidence, environmental indicators, and bodily changes.

Circumstantial evidence such as when the deceased was last seen alive, etc., can certainly be helpful to narrow down PMI, but certainly not universal to all cases, and can be confounded by many variables influencing bodily changes; as this is not part of forensics per se, we will not comment on the use of circumstantial evidence any further. Environmental indicators of PMI include external processes such as forensic entomology, the study of insects such as flies that parasitize dead tissue^{7,8}. In that case, insects may lay eggs on mucous membranes such as eyes or mouth, which later develop into larva. By studying eggs and larva, an entomologist may estimate the earliest time that egg laying occurred that, under ideal circumstances, can suggest the minimum PMI. However, maximum PMI cannot be estimated using this approach, which is also confounded by environmental temperatures that influence egg hatching and larva development, and are precluded if the corpse exists in an environment with few to no insects.

Postmortem bodily changes are perhaps the best studied and most useful ways to estimate PMI that we have today, and refer to how a corpse is impacted by different physical, biochemical, and biological processes⁹. The

¹Department of Physics and Astronomy, University of Calgary, Calgary, Canada. ²Department of Surgical Sciences, Uppsala University, Uppsala, Sweden. ³Swedish National Board of Forensic Medicine, Stockholm, Sweden. ⁴Robson DNA Science Centre, Arnie Charbonneau Cancer Institute, Department of Biochemistry and Molecular Biology, Department of Oncology, Cumming School of Medicine, University of Calgary, Calgary, Alberta, Canada. ⁵Occupational and Environmental Medicine, Department of Medical Sciences, Uppsala University, Uppsala, Sweden. ⁶Occupational and Environmental Medicine, Uppsala University Hospital, Uppsala, Sweden. ✉email: behnam.ashrafkhan1@ucalgary.ca

classic early signs of death are livor mortis, rigor mortis and algor mortis³. Livor mortis is the collection of blood in dependent parts of a body due to the cessation of circulation, leading to a blue-reddish discoloration of the skin which usually starts to appear within an hour after death. Rigor mortis is stiffening of muscles due to energy depletion and usually begins to form around three hours postmortem. However, both Livor mortis and Rigor mortis are confounded by known and unknown factors, and their presence or absence can only be used to make crude assessments of the PMI. Algor mortis refers to the gradual cooling of the body from 37°C to ambient temperature, is predictable under certain circumstances, and it is the most used method of PMI assessment if a corpse is found within hours of death. Algor mortis can be used up within 24–48 hours postmortem, depending on person's weight and clothing, and if the ambient temperatures are 20°C. In optimal cases, the Henssge's nomogram¹⁰ gives a PMI estimation of PMI ±2.8 h within 95 percent confidence interval (CI₉₅). However, the reliability of algor mortis is confounded by temperature extremes, hypo- or hyperthermia, sunlight exposure, clothing, if the corpse is wet or dry, movement of air, and crime scene variables such as opening doors or windows, or the body being covered by a blanket. Another bodily change measurement used for PMI estimation is to evaluate the gradual rise in potassium concentration in vitreous fluids after death¹¹, although this has a margin of error in hours to days depending on formulae used¹². Finally, the rate of decomposition caused by autolysis (self-digestion by endogenous enzymes) and putrefaction (digestion by micro-organisms) can be useful, although is accelerated by high ambient temperature, fever, and/or sepsis, is delayed by cold, and generally has uncertainties so large its use is questioned in court^{9,13}.

Of all the PMI methods, body temperature and vitreous potassium are best studied and of most use². That said, both approaches have drawbacks in that they require certain environmental conditions, come with large margins of error, or have a relatively short time window in which they can be used. Because of this, investigators have been exploring different bodily change analytes or parameters to find 'something better'. However, some forensic medicine authorities have speculated that this search does not make any sense, since parameters for existing bodily changes would also change with increasing PMI and be influenced by the existing confounding factors such as ambient temperature¹⁴. Henssge and Madea¹⁴ offered the opinion that new PMI methods "only gain practical relevance if the following criteria are fulfilled: quantitative measurement, mathematical description, taking into account influencing factors quantitatively, declaration of precision and proof of precision on independent material"¹⁴. Hence, the challenge is to overcome the underlying problem with the classical forensic PMI methods: that they depend on parameters that show inherently wide variations dependent on too many variables. No matter how large studies are, these variations will still be there and it is not possible to include all possible internal and environmental conditions.

The motivation for our study was to ideate a tool that is independent of biological processes or environmental circumstances and, instead, is based on a well-characterized process that depends only on atomic physical properties such as radioisotopic stability. In this context, the application of a short-lived radioactive decay chain is appropriate since the probabilities of nuclear decays are innately independent of environmental conditions such as temperature, pressure, humidity, or biology. Radioactive decay has been studied for PMI estimation before^{15–17}, with the best-studied and most used method being carbon-14 (¹⁴C) analysis used by archaeologists to date skeletal remains. In 1998, Benjamin Smith proposed using the ratio of radioactive lead-210 (²¹⁰Pb) and polonium-210 (²¹⁰Po) to date skeletal remains of interest to forensic anthropology, although it was considered impractical at the time¹⁶. More often, and thanks to radioactive strontium-90 (⁹⁰Sr) contamination of the atmosphere from 20th century atomic weapon testing, ⁹⁰Sr pulse measurement is now used to date human skeletal remains, albeit with error in the range of years^{18,19}. Of all these radioisotopic methods, none are considered practical for estimating PMI with the sensitivity needed to be of use to active forensic cases, where timelines must be measured in hours instead of decades.

For radioactive decay to be useful in ordinary forensic PMI investigation, we suggest the following prerequisites need to be fulfilled. First, the parent radioisotope must be present in a majority (or all) dead bodies regardless of location or medical history. Second, the measurements must be sensitive enough to detect reliable changes in the amounts of the radioactive parent and its decay products over the PMI of interest, usually days to weeks, or perhaps months depending on the case. Third, investigators must be able to calculate the amount of the radioactive element, and its decay products present in the body at the time of death, or there must be a predictable (ideally universal) development of the subsequent ratios for isotopes in life and after death.

We hypothesize that measuring the numerical ratio between a radioisotope and its decay products could meet these criteria and become a helpful new way to derive PMI. For example, if one observes that isotope A decays to stable isotope B with a half-life of one day, a ratio of A:B of 1:1 would mean that the body has been dead for a day, assuming that there was no amount of B at the time of death. Here, we discuss and investigate a theoretical forensic system that is ubiquitous amongst the human population, naturally present in the terrestrial environment, and would not rely on understanding specific medical histories of individuals.

Results

Conceptual framework

We speculate that there is an opportunity to estimate PMI using the relative abundance of radioactive decay products generated from naturally occurring ²²²Rn and that is absorbed by living systems. More specifically, the inhalation of radon gas and its decay products is functionally universal on Earth, as ²²²Rn is generated by uranium isotope-bearing minerals within the lithosphere and migrates via free-phase gas and water to the surface, where it enters the atmosphere of including indoor and outdoor air environments occupied by people^{20,21}. Human populations are exposed to some amount of radon and radon decay products daily, which is typically measured in an indirect manner by evaluating the amount of alpha particle emissions per second (Bq) per cubic metre of air (Bq/m^3)²². ²²²Rn levels in outside air are typically measured in the 1–60 Bq/m^3 range^{23–25}, although can be > 100 Bq/m^3 in exceptional cases²⁶. Indoor air or subterranean air radon amounts

can be anything from 10–100,000 Bq/m^3 , depending on building and region²⁰. ^{222}Rn has a relatively short half-life of 3.8 days before undergoing a series of radioactive decays to form a series of very short lived ($t_{1/2}$ = microseconds to minutes) isotopes of Po, Pb and Bi before becoming long-lived ($t_{1/2}$ = 22.3 years), then ^{210}Bi ($t_{1/2}$ = 5 days), ^{210}Po ($t_{1/2}$ = 138 days), and finally stable ^{206}Pb (Figure 1).

Although exposure to some amount of gaseous ^{222}Rn and solid radon decay products is functionally universal, the specific amount of these radioisotopes inhaled by a person occurs at variable amounts across a lifetime depending on where they live, in what buildings they occupy, and behavioural factors such as occupation, tobacco use, diet and more^{27–31}. It is important to understand that human exposure to radon and its decay products is a function of how much gaseous ^{222}Rn is constantly entering a given environment from geogenic sources, and also those radon-decay products that have equilibrated within the same environment via ^{222}Rn decay and attachment to particulates such as smoke or dust²⁰. Both gaseous radon and the ‘attached fraction’ of radon decay products are inhaled and will be absorbed into living tissue via the lungs^{32–34}. To a lesser extent, radon and its decay products can be ingested via drinking groundwater, eating certain foods such as ^{210}Pb -rich lichen-eating wild game (e.g. caribou, elk, deer, moose), or tobacco smoking^{34–36}. As all these routes of exposure demand that a person is alive, the deposition of ^{222}Rn and radon decay products within tissue is innately associated with life, whilst the cessation of breathing, drinking, and/or eating that occurs at death marks the end of incoming ^{222}Rn and radon decay products.

Careful measurement of the relative abundance of these decay products is now possible using recent advances in technology and so, for the first time, it is theoretically possible to use a radioisotopic decay of ^{222}Rn to evaluate PMI. Indeed, previous work by Ziad and colleagues³⁷ explored the use of radon decay product ratio measurements to estimate time of death. Assumptions made during that investigation included constant radon exposure during life and an initial equilibrium value of ^{210}Pb : ^{210}Po that complicates time of death estimation³⁷; as these assumptions were undefined, they added uncertainties. We note that while the theoretical idea to measure ^{222}Rn decay products to estimate PMI is straightforward, its practical application is not. The accumulation of radon decay products in tissue is in the order of femtogram per gram (fg/g). Consequently, hypersensitive instruments are needed to measure isotope abundance (*i.e.* number of atoms) of radon decay products in biological tissues. If a low abundance measuring procedure is in place, as has been achieved for uranium or plutonium isotopes³⁸, the next problem is to identify tissues that are helpful to measure within the context of a corpse, based how radon decay products are stored in the body. Current evidence suggests that, in addition to the lungs, keratinizing tissue (nails), adipose tissue (fat), and bone are all tissues where radon decay products have been empirically found to accumulate^{33,34}. To develop and evaluate a theoretical model, we divided our work into two consecutive phases: the forward model and the actual Radon Time of Death Clock calculation. Our rationale was to use the radioactive decay equations under the assumption of a steady source of radon to generate data that could then be used to test the accuracy of the Radon Time of Death Clock. A critical component of the Radon Time of Death Clock developed here is the use of (1) relative numbers of isotopes and (2) two pairs of isotope abundance ratios. These input data enable a determination of the elapsed time since death to very high accuracy and is a key feature of this approach.

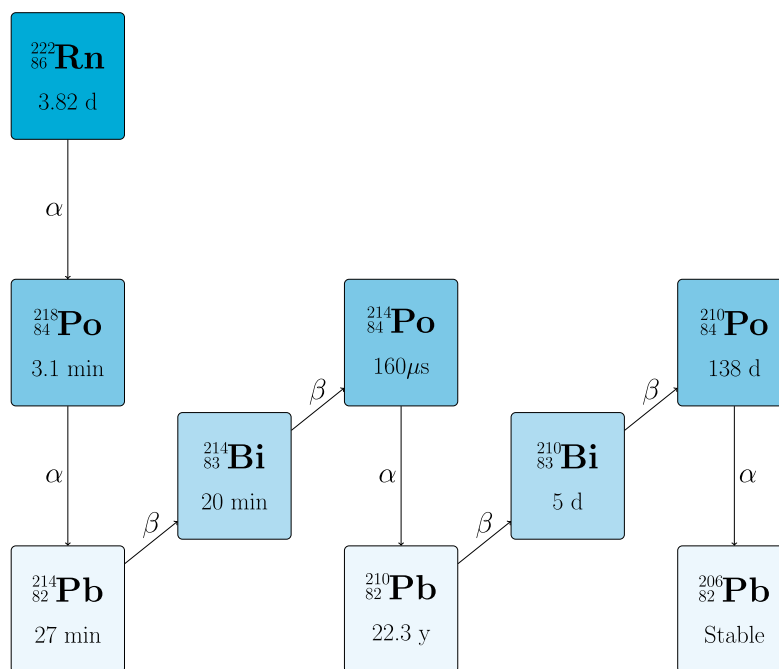


Fig. 1. The ^{222}Rn main decay chain and daughter products. The half-life of each isotope is indicated. Only the dominant decay pathways are shown and low-probability branches (e.g., ^{218}Po to ^{218}At) are omitted for clarity.

The forward model

For the forward model, we conceptualized a person who inhaled air containing an average of 100 Bq/m^3 radon from birth to the time at which they died (time of death = t_d). The radon exposure assumption reflects the reality of radon in many nations including, for example, Canada where recent outcomes of national surveying found that the geometric mean, weighted level of radon in a residential building is 84.7 Bq/m^3 , with 42% of people experiencing levels of radon 100 Bq/m^3 or more. For the forward model, we also assumed inhalation of radon and all radon decay products ceased entirely at the time of death, and that the numbers of ^{210}Pb , ^{210}Bi , and ^{210}Po atoms each began to decrease according to radioactive decay laws and their respective radioisotopic decay probabilities. At specific times after the discovery of the theoretical corpse by investigating authorities, we assumed the measurements of radon decay products in one or more tissues from the body could be performed (time of measurement = t_m), including the numbers of remaining atoms and isotope number ratios.

We suggest that two ratios that involve three radon decay isotopes (^{210}Pb , ^{210}Bi , and ^{210}Po) are of particular interest, as these isotopes have relatively longer half-lives; these ratios are: $r_1 = \frac{^{210}\text{Pb}}{^{210}\text{Po}}$ and $r_2 = \frac{^{210}\text{Pb}}{^{210}\text{Bi}}$. Starting with zero atoms for all the species of interest, and having a set of decay rates, we can obtain the ratios of the number of atoms at any time before or after death. The decay equations guarantee existing a unique set of ratios for any specific set $\{t_d, t_m\}$,

$$\begin{aligned} dN_0t &= A - \lambda_0 N_0, \\ dN_1t &= \lambda_0 N_0 - \lambda_1 N_1, \\ dN_2t &= \lambda_1 N_1 - \lambda_2 N_2, \\ dN_3t &= \lambda_2 N_2 - \lambda_3 N_3, \end{aligned} \quad (1)$$

In this scenario, the value A (Bq) represents the constant activity level of radon in air, and (λ_0, N_0) , (λ_1, N_1) , (λ_2, N_2) , (λ_3, N_3) denote decay constants and number of atoms for ^{222}Rn , ^{210}Pb , ^{210}Bi and ^{210}Po , respectively. However, after death, the first equation follows:

$$dN_0t = -\lambda_0 N_0, \quad (2)$$

In this scenario, the supply of radon to the body ceases, the ^{222}Rn atoms undergo decay and, since the person is no longer inhaling air, there is no source to replenish the ^{222}Rn atoms. Below are the solutions to the above equations before death:

$$N_1(t) = \frac{A\lambda_0(1 - e^{-\lambda_1 t})}{\lambda_1}, \quad (3)$$

$$N_2(t) = \frac{A\lambda_0(\lambda_1(1 - e^{-\lambda_2 t}) + \lambda_2(e^{-\lambda_1 t} - 1))}{(\lambda_1 - \lambda_2)\lambda_2}, \quad (4)$$

$$\begin{aligned} N_3(t) &= \frac{A\lambda_0 e^{-(\lambda_1 + \lambda_2 + \lambda_3)t}}{(\lambda_1 - \lambda_2)(\lambda_1 - \lambda_3)(\lambda_2 - \lambda_3)\lambda_3} \times [(\lambda_1^2 e^{\lambda_1 t} (\lambda_2 e^{\lambda_2 t} (e^{\lambda_3 t} - 1) - \lambda_3 e^{\lambda_3 t} (e^{\lambda_2 t} - 1)) \\ &\quad + \lambda_1 e^{\lambda_1 t} (\lambda_3^2 e^{\lambda_3 t} (e^{\lambda_2 t} - 1) - \lambda_2^2 e^{\lambda_2 t} (e^{\lambda_3 t} - 1)) \\ &\quad + \lambda_2(\lambda_2 - \lambda_3)\lambda_3 e^{(\lambda_2 + \lambda_3)t} (e^{\lambda_1 t} - 1)]. \end{aligned} \quad (5)$$

A Monte Carlo simulation was done where the age of the individual and the time that elapsed between death (t_d) and the measurement (t_m) were varied. Specifically, t_d varied between 20 and 40 years and t_m varied up to 20 days. The simulation was run 3,500 times to create multiple sets of $\frac{^{210}\text{Pb}}{^{210}\text{Bi}}$ and $\frac{^{210}\text{Pb}}{^{210}\text{Po}}$ isotope number ratios, with each pair having a known t_d and t_m .

The radon time of death clock

We next used the data generated from Monte Carlo simulations as input quantities to the Radon Time of Death Clock, to test its theoretical accuracy, meaning how well outcomes predicted a known time of death. The calculation of the elapsed time for measuring the numbers of ^{210}Pb , ^{210}Bi , and ^{210}Po atoms (t_m) was based only on the relative isotope number ratios. Thus, the input quantities to the Radon Time of Death Clock were the r_1 and r_2 ratios. Here, we assumed the individual was exposed to a constant level of radon over their lifetime. The model was implemented in Python 3.0 and employs the “brute force” method that involved calculating the function’s value at each point on a multidimensional grid to determine the function’s global minimum, and the Nelder-Mead minimization algorithm to calculate the elapsed times between death and measurement of isotopic composition.

The model solved the radioactive decay equations simultaneously for the two pairs of number ratios such that, although the radioactive decay probabilities for each radionuclide are different, the elapsed time for radioactive decays must be the same. Very importantly – as it would be impractical in the field – knowledge of the absolute radon exposure of the person at the time of death was not needed, as this quantity was cancelled out in the calculation since equations employed the relative number of isotopes (*i.e.* ^{210}Pb to ^{210}Bi and ^{210}Pb to ^{210}Po). The use of two sets of the relative numbers of isotopes enabled the calculation of a unique answer. In the case of using a single isotope number ratio in the calculation (*i.e.* only ^{210}Pb to ^{210}Bi), the result from the model was not unique. However, if both relative isotope number ratios were input to the model, then the result was

constrained to a much narrower range of possible values for the time elapsed between death and measurement, where a solution to the equations is found.

Constant lifetime radon exposure

In the hypothetical scenario of constant radon exposure during a lifetime, we define a two-dimensional vector field, $\vec{r} = \vec{S}(t_d, t_m)$, where $\vec{r} = (r_1, r_2)$. Vector field \vec{S} can be evaluated based on decay equations for any valid set $\{t_d, t_m\}$, either analytically or numerically. We consider evaluating vector field \vec{S} at any given time set to be 'solving the direct problem' – i.e., solving the direct problem simulates a reality in which a person lived for a specific time with a constant radon exposure, died at t_d , and the r_1 and r_2 ratios are measured at $t_d + t_m$. The components of $\vec{S}(t_d, t_m)$ give us the ratio values in the ideal case of no uncertainty in the measurement results.

Assuming that there is a unique set of times, $\{t_{d,T}, t_{m,T}\}$, which leads to a specific set of measured ratios, $\{r_{1,T}, r_{2,T}\}$ (i.e. $\vec{r}_T = (r_{1,T}, r_{2,T}) = \vec{S}(t_{d,T}, t_{m,T})$) that we define 'solving the inverse problem' as follows. The subscript T denotes the true value, which is presumed to be measured. Due to the absence of uncertainty, this true value should correspond to the value obtained from the forward model. When defining the scalar field,

$$E_{\vec{r}_T}(t_d, t_m) = \left| \vec{S}(t_d, t_m) - \vec{r}_T \right|, \quad (6)$$

we suggest that there should be one single global minimum for $E_{\vec{r}_T}$ which happens at $(t_{d,T}, t_{m,T})$. Hence, for a given set of valid ratios, \vec{r}_T , one can find the set of times, $\{t_{d,T}, t_{m,T}\}$, that leads to the measured ratios, by minimizing the scalar field $E_{\vec{r}_T}$.

To test the accuracy of the model, we next calculated the elapsed time since death for the isotope pairs produced by the Monte Carlo simulations. The results are shown in Figure 2a, where the difference between actual and calculated elapsed measurement times (optimization error) are plotted as a function of the time that has elapsed since death. Outcomes demonstrate that the Radon Time of Death Clock could provide reliable results within just a two-week window after actual the death of the individual, and were remarkably precise with the average absolute error of 114 milliseconds. The consistency of the results was supported by a standard deviation of approximately 141 milliseconds. The error distribution arising from a scenario involving constant radon exposure and a single time measurement of two isotope pairs is shown in Figure 2b.

Accounting for variation in radon exposure across a lifetime

In reality, people are exposed to ^{222}Rn and solid radon decay products at a variable rate and at different levels across their lifespan^{20,21,28,39}. Empirical evidence for ever changing radon exposure across a lifetime exists and has been demonstrated, with shifts in exposure caused by life events such as entering the workforce, changing profession, starting or stopping tobacco smoking, moving house, entering retirement, obtaining a radon reduction, and/or more systemic events such as implementation of pandemic emergency lockdown responses telecommuting, or nation wide building code changes^{27–31}. So, to make the model more realistic, we next modeled a scenario where we assumed that the rate of radon exposure undergoes multiple changes during individual's lifespan (albeit, for simplicity, each period of exposure was constant between jumps).

Similar to the case of constant exposure, we define the vector field $\vec{r} = \vec{S}_{f(t)}(t_d, t_m)$, where $f(t)$ is a piece-wise constant function of time that gives the overall rate of radon exposure activity over time. Note that the rate of radon exposure activity is defined only within the time between conception and death and that, after death, all relevant radionuclides will decay with no further input from parental ^{222}Rn and/or solid radon decay products. Therefore, all the discontinuities of $f(t)$ should satisfy $0 < t < t_d$, and $f(t) = 0$ for $t > t_d$. Furthermore, for a constant function $f(t)$ within $0 < t < t_d$, we have, $\vec{S}_{f(t)} = \vec{S}$. Mathematically, we define,

$$f(t) = \begin{cases} a_1 & , 0 < t < t_1 \\ a_2 & , t_1 < t < t_2 \\ \vdots & \\ a_N & , t_{N-1} < t < t_N \\ a_{N+1} & , t_N < t < t_d \\ 0 & , t_d < t \end{cases}, \quad (7)$$

Here, N is the number of jumps in the rate of radon exposure activity the person experiences, while $t_n \in T_{jumps}$ is the time of n^{th} jumps, and $a_j \in jumps$ is the constant value describing the rate of radon exposure activity between two successive jumps.

In an ideal scenario, solving the inverse problem would determine the set of parameters $\{t_d, N, jumps, T_{jumps}, t_m\}$, in which N is the number of jumps, $jumps$, is the set of activity values between the jumps, and T_{jumps} is the set of times of jumps before t_d , such that these lead to a set of ratios that match with the measured values in reality (or the outcome of $\vec{S}_{f(t)}(t_d, t_m)$). However, from a practical perspective, solving such a problem would far too computationally expensive to be helpful (i.e., impractical using regular computers, as the number of unknown parameters is large). It can be claimed that if there is any piece-wise constant function $\hat{f}(t) \neq f(t)$ and $\hat{t}_d \neq t_d$ such that,

$$\vec{S}_{\hat{f}(t)}(\hat{t}_d, 0) \simeq \vec{S}_{f(t)}(t_d, 0), \quad (8)$$

Then will have the equation below for any t_m :

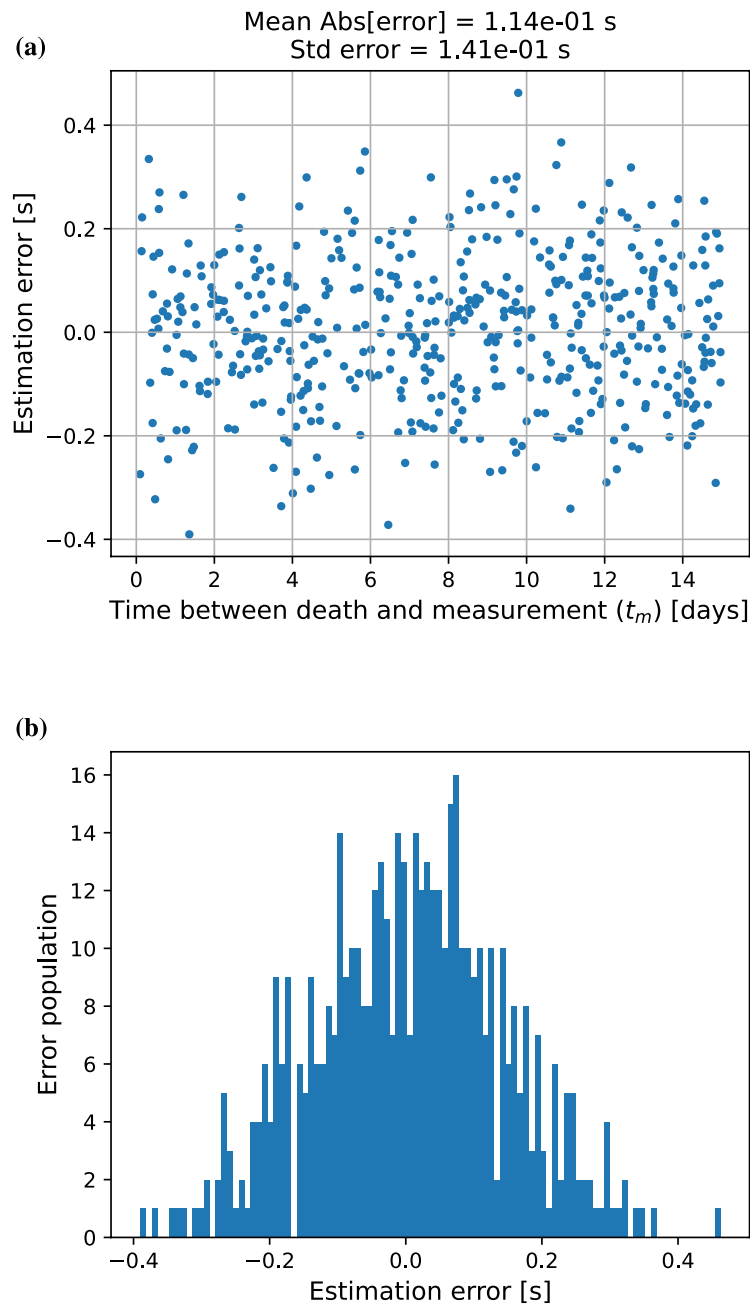


Fig. 2. (a) Difference between the true and calculated elapsed time since death using the two pairs of isotope number ratios. Note that no uncertainty was assumed for the input quantities to the model. The RTDC could calculate the accurate time of death to within seconds. (b) Distribution of errors in post-mortem interval estimation under constant radon exposure conditions, showing Gaussian distribution pattern of discrepancy between predicted and actual time since death.

$$\vec{S}_{\bar{f}(t)}(\bar{t}_d, t_m) \simeq \vec{S}_{f(t)}(t_d, t_m), \quad (9)$$

The implication of this is that the post-mortem evolution of these radioisotopic ratios is predicted to follow a similar pattern regardless of the lifespan or lifetime radon exposure of the person, meaning this readout of PMI is agnostic to inter-individual differences, and so is likely helpful to forensic investigators who need to ascertain PMI. To move forward with evaluation our model, we proceeded under the assumption that it is feasible to replicate the post-mortem characteristics of r_1 and r_2 from a scenario with the death occurring at time t_d and multiple fluctuations in the rate of radon exposure activity over the lifespan. We used a less complex scenario where death happens at a different time t'_d ($t_d \neq t'_d$) and involves a single change in rate of radon exposure activity. Although this approach is an approximation and will not exactly mirror the reality of lifetime radon

exposure, it is a reasonable estimation for a wide range of cases. To formulate the aforementioned approximation, we initially define a step-function $g(t)$ as follows,

$$g(t) = \begin{cases} a_1 & , 0 < t < t_1 \\ a_2 & , t_1 < t < t_d \\ 0 & , t_d < t \end{cases} . \quad (10)$$

Since we deal with the ratios, the absolute values of a_1 and a_2 do not affect the results directly, rather, the ratio $a = a_2/a_1$ is what is important for us. So, we redefine the function $g(t)$ to reduce the number of parameters,

$$g(t) = \begin{cases} 1 & , 0 < t < t_1 \\ a & , t_1 < t < t_d \\ 0 & , t_d < t \end{cases} . \quad (11)$$

Now, with having $\vec{r}_T = \vec{S}_{f(t)}(t_{d,T}, t_{m,T})$, we define the scalar field,

$$E_{\vec{r}_T}(t_d, t_m, t_1, a) = \left| \vec{S}_{g(t)}(t_d, t_m) - \vec{r}_T \right|. \quad (12)$$

Similar to the case of constant activity, by minimizing the scalar field $E_{\vec{r}_T}$, we can obtain the set of parameters that result in the ratios of interest, and those parameters include t_m .

Measurement of radioisotope ratios at multiple times postmortem

The theoretical approach we have described so far yields generally satisfactory outcomes. However, in certain instances, we observed that it can lead to very large uncertainty on t_m values. The discrepancy arises because the parameters $\{t_d, t_m, t_1, a\}$ that result in \vec{r}_T are not unique, and an example where the method fails is depicted in Figure 3.

In all cases, the resulting ratios match those obtained from the forward model simulation. However, there is a notable discrepancy in the estimation of t_m . To address this issue, one approach we suggest is to incorporate radioisotope ratios with their rates of change (time derivative) into the analysis. As an approximation of the time derivative, a second measurement of ratios can be introduced into the scenario. The first measurement takes place at $t_{1,T} = t_{d,T} + t_{m,T}$, and the second measurement at the time $t_{2,T} = t_{d,T} + t_{m,T} + t_{\text{step}}$. The outcomes are denoted as $\vec{r}_{1,T} = (r_{1,1,T}, r_{2,1,T})$ for the first measurement and $\vec{r}_{2,T} = (r_{1,2,T}, r_{2,2,T})$ for the second one.

$$\vec{r}_{1,T} = \vec{S}_{f(t)}(t_{d,T}, t_{m,T}), \quad (13)$$

$$\vec{r}_{2,T} = \vec{S}_{f(t)}(t_{d,T}, t_{m,T} + t_{\text{step}}). \quad (14)$$

Then we define the scalar field that should be minimized as,

$$E_{\vec{r}_{1,T}, \vec{r}_{2,T}}(t_d, t_m, t_1, a) = \left| \vec{S}_{g(t)}(t_d, t_m) - \vec{r}_{1,T} \right| + \left| \vec{S}_{g(t)}(t_d, t_m + t_{\text{step}}) - \vec{r}_{2,T} \right|. \quad (15)$$

The error distribution for a model with varying radon exposure and two measurements of two isotope pairs that are separated in time is in Figure 4. Since no measurement of isotopic composition is free from uncertainty, a preliminary study was carried out to explore the sensitivity of the Radon Time of Death Clock to measurement errors. An initial run introduced random error to the the r_1 and r_2 isotope number ratios and the model calculations were repeated using a relative standard deviation of 0.01 percent in the ratios. Under these conditions, the uncertainty in the elapsed time calculation increased to approximately 1 day. To explore the theoretical limit of the model's temporal resolution, calculations were repeated assuming a relative uncertainty of 0.01% in the isotope ratios. While this level of precision is not currently achievable using standard detection techniques, it serves as an upper-bound scenario to evaluate model behavior under idealized conditions, such as might become accessible through future advances in measurement technology.

Discussion

In this study, we explore the idea of estimating near-term PMI by analyzing radioactive radon decay products, building upon radiometric forensic science and earlier work within the context of forensic anthropology¹⁶. Our model's potential lies in its utilization of isotope abundance ratios of ^{210}Pb and ^{210}Po before equilibrium is reached. By measuring two isotope abundance ratios of the ^{222}Rn decay products from a sample at different points in time after death, the technique allows for accurate determination of the PMI. At this stage, we consider the approach of using two pairs of isotope number ratios to solve the radioactive decay equations to be effective at estimating the elapsed time between death and measurement to a practical level of uncertainty. Important open questions remain, including the impact of variable radon and radon decay product exposure levels (across a lifetime) on the results. There is also the critical challenge of measuring the numbers of ^{210}Pb , ^{210}Bi and ^{210}Po with sufficient precision and accuracy such that the model can produce reliable results; this is a subject of ongoing research to develop the necessary analytical methods and hypersensitive tools needed to achieve this objective.

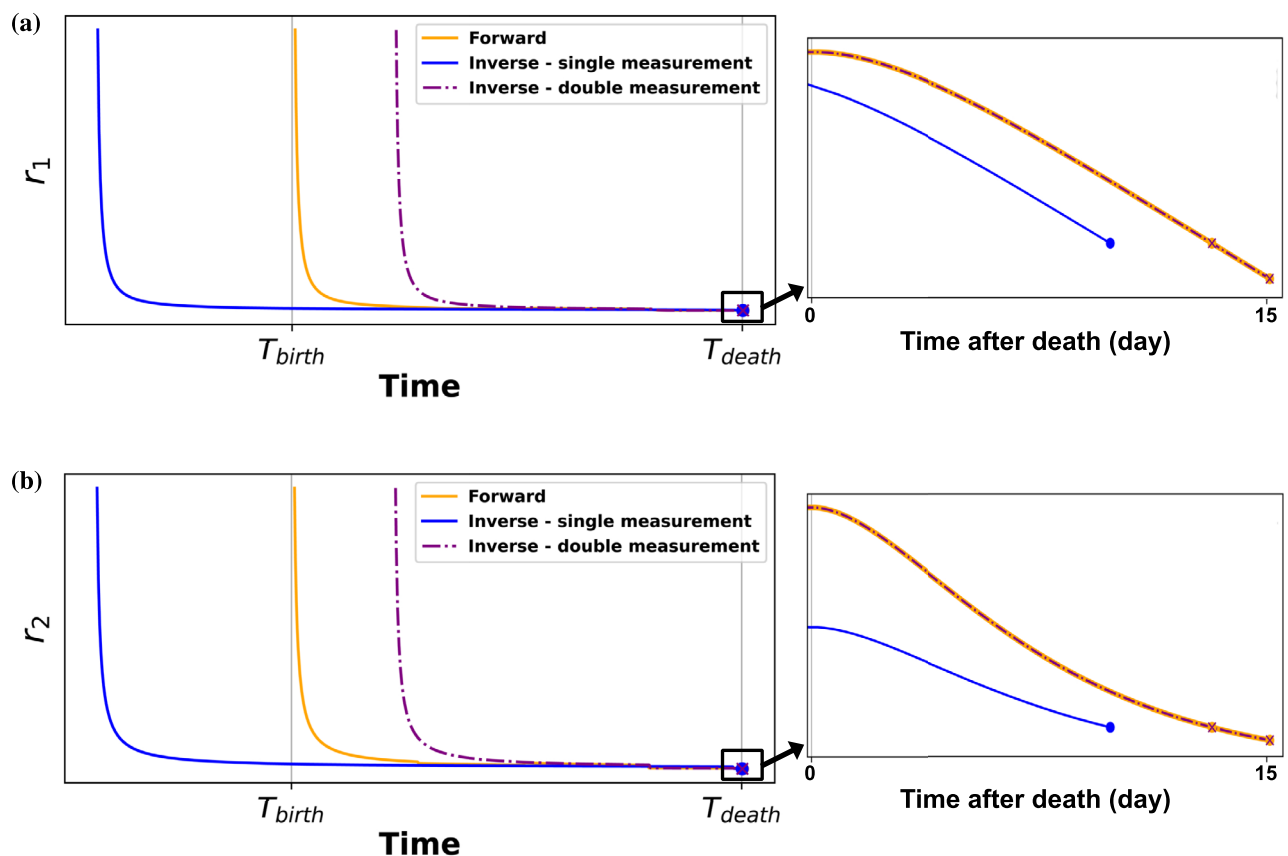


Fig. 3. This figure demonstrates how minimization is used to estimate the time of death based on forward model data. A single postmortem measurement, which did not match accurately the true time of death, was also analyzed using double measurement approaches. Under lifetime-varying radon exposure, the minimization curve deviates from the forward model (true ratio curve) when using a single postmortem measurement. In contrast, the dashed line representing the double measurement approach closely matches the forward model. **(a)** shows the minimization result for isotope ratio r_1 ($\frac{^{210}\text{Pb}}{^{210}\text{Po}}$) and **(b)** the minimization result for isotope ratio r_2 ($\frac{^{210}\text{Pb}}{^{210}\text{Bi}}$).

A limitation of the present study lies in the absence of empirical validation using postmortem biological samples. While the theoretical model demonstrates mathematical precision and internal consistency, its real-world forensic applicability depends on the ability to measure the abundances of ^{210}Pb , ^{210}Bi and ^{210}Po in tissue samples postmortem, and to confirm that the modeled assumptions hold under biological and environmental variability. We acknowledge that future experimental studies are essential to validate the model predictions and assess the feasibility of implementing the approach under operational forensic conditions. As a first step toward this goal, we are developing a validation plan using postmortem animal tissue (e.g., rat lungs) to simulate realistic decay scenarios under controlled conditions. For the measurement of radon progeny at trace levels, we aim to employ laser ionization coupled to multiple-reflection time-of-flight mass spectrometry (MR-TOF-MS) at the TITAN facility at TRIUMF⁴⁰, which offers the required mass resolving power and was specifically designed for the selective detection of low-abundance radionuclides. Incorporating experimental results will be a critical next step in translating this computational framework into a forensic tool.

A key advantage of the framework we propose is its ability to determine PMI without requiring knowledge of a person's lifetime radon exposure level – which would be impractical. We have tested models that assume a constant radon exposure level, a scenario that cancels out needing to know lifetime radon exposure within decay equations. The simplification enables accurate PMI estimation regardless of the specific exposure value, as long as it remains constant and, under ideal conditions, this approach can predict the PMI with less than 0.5 seconds precision – a good starting point. In realistic scenarios where the rate of radon exposure varies over an individual's lifetime, the model can still estimate the postmortem interval (PMI) within 10 minutes – an additional advantage, especially when considering the variability and confounding factors that affect current PMI estimation methods. To estimate t_m in cases where radon exposure varies over a person's lifetime, we approximate the postmortem behavior of isotope ratios using a simplified model that assumes a single radon exposure jump during life (Eq. 9). For this approximation to be valid, not only must the isotope ratios in the

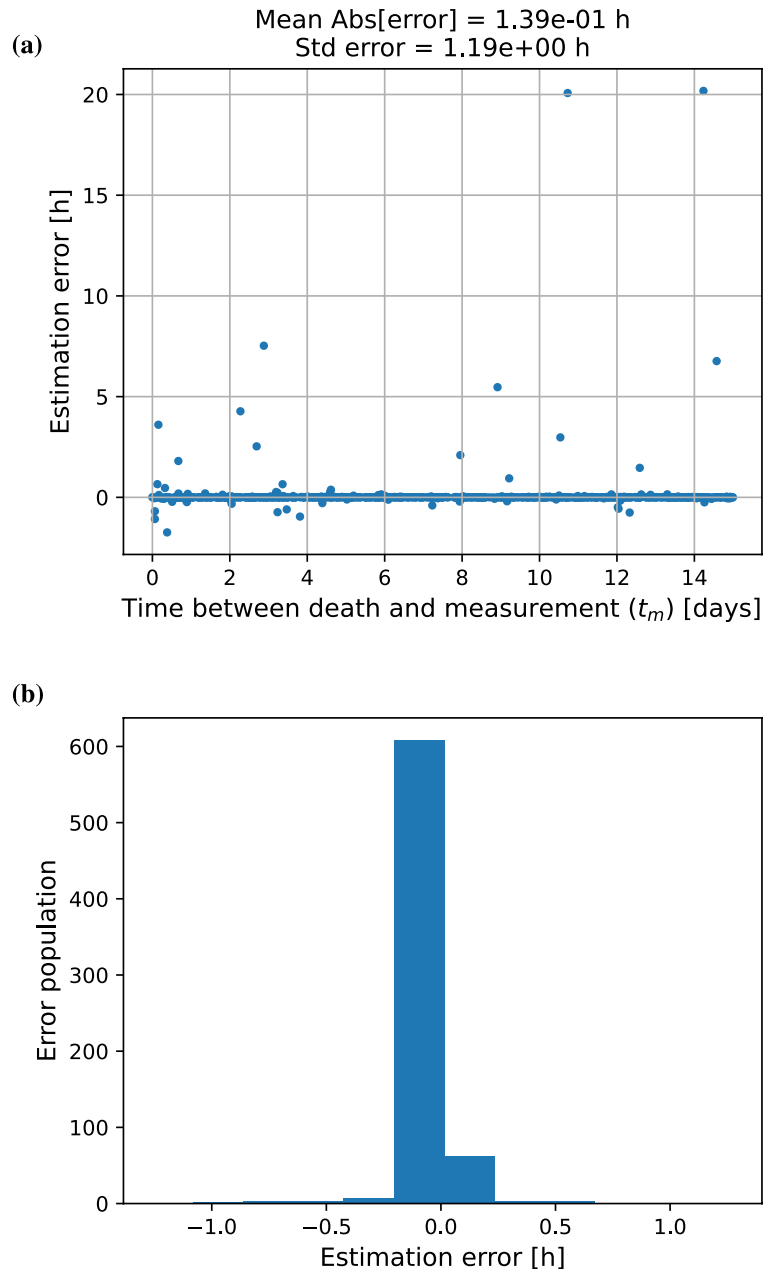


Fig. 4. (a) Difference between the true and calculated elapsed time since death using two pairs of isotope ratios. The study employed a double measurement approach, where two pairs of isotopes were measured twice at separate time intervals. Note that no uncertainty was assumed for the input quantities to the model. The RTDC could calculate the accurate time of death to within 10 minutes. (b) Distribution of optimization errors in post-mortem interval estimation under varying radon exposure conditions, showing Gaussian distribution pattern of discrepancy between predicted and actual time since death.

actual and simplified cases match at the time of death (Eq. 8), but their time derivatives of all orders must also match. Such a requirement arises from the principle of Taylor expansion, where a function can be reconstructed from its value and all derivatives at a single point. In practice, matching all time derivatives is generally not feasible with the available information. These findings highlight three important aspects. First, the postmortem isotope abundance ratios ($^{210}\text{Pb}/^{210}\text{Bi}$ and $^{210}\text{Pb}/^{210}\text{Po}$) change dynamically over time, particularly in the first few days or weeks after death. Second, a single ratio measurement can lead to ambiguities or non-unique solutions when lifetime exposure is variable. Third, adding a second postmortem measurement enables the model to numerically approximate the rate of change (the time derivative) of the ratios, which significantly improves the accuracy and uniqueness of the solution. However, the method becomes valid under a specific condition, when the ratios are in equilibrium at the time of death – that is, when their time derivatives approach zero. In such cases, the dynamic behavior of the ratios after death can be reconstructed based solely on their values at the time

of death. Therefore, equilibrium at the time of death is a necessary condition for reliably estimating t_m using this simplified model. If a change in radon exposure occurs shortly before death (e.g., within the final year or two of life) and disrupts this equilibrium, the method becomes inefficient for estimating the postmortem interval.

It is important to consider that there are a wide variety of emerging approaches that are being explored today to estimate PMI in a way that is useful for active case forensics. These emerging approaches include use of lipidomics, proteomics, and/or metabolomics to evaluate biochemical changes within dead tissues such as organs, bones, blood, etc.⁴¹. Other techniques that measure DNA, RNA or protein degradation within a corpse are also being evaluated for efficacy^{42–44}, and there exists a compelling case for monitoring the “necro-microbiome”, meaning micro-organisms of the Bacillota and Pseudomonadota phyla that are prevalent within the body during postmortem periods, and that can be evaluated using next generation DNA sequencing methods⁴⁵. We note that the same confounding variables that complicate existing biological approaches to PMI estimation - especially ambient temperature and the health status of the person prior to death - still apply to all newly emerging biological approaches. By contrast, analyzing radioactive decay to estimate PMI is innately independent of the environmental and biological factors that negatively affects the reliability of other PMI methods.

The method we propose fulfills the criteria that has been called for by forensic science authorities in terms of being quantitative, having a mathematical description, and accounting for confounding variables in a quantitative manner. The observed agreement between the calculated and actual elapsed times indicates that the approach has potential for reliable (precise and accurate) PMI estimation. We suggest that the next step in evaluating whether this approach can be implemented is to design a comprehensive analytical procedure to systematically evaluate the algorithm's performance, optimize its parameters, and ensure its robustness across various conditions.

Data availability

The datasets generated and/or analysed during the current study are available in the GitHub repository: <https://github.com/BehnamAsh/RTDC>

Received: 23 June 2025; Accepted: 6 August 2025

Published online: 09 August 2025

References

- Ruiz López, J. L. & Partido Navadizo, M. Estimation of the post-mortem interval: a review. *Forensic science international* **369**, 112412 (2025).
- Wenzlow, N., Mills, D., Byrd, J., Warren, M. & Long, M. T. Review of the current and potential use of biological and molecular methods for the estimation of the postmortem interval in animals and humans. *Journal of Veterinary Diagnostic Investigation* **35**, 97–108 (2023).
- Madea, B. *Handbook of Forensic Medicine* (John Wiley & Sons, Incorporated, Newark, 2014), 1 edn.
- Sutton, L. & Byrd, J. An introduction to postmortem interval estimation in medicolegal death investigations. *WIREs Forensic Sci.* **2**, e1373, <https://doi.org/10.1002/wfs2.1373> (2020).
- Garcés-Parra, C. et al. Enhancing late postmortem interval prediction: a pilot study integrating proteomics and machine learning to distinguish human bone remains over 15 years. *Biol. research* **57**, 75–15 (2024).
- Matuszewski, S. Post-mortem interval estimation based on insect evidence: Current challenges. *Insects (Basel, Switzerland)* **12**, 314 (2021).
- Hu, G. et al. A global perspective of forensic entomology case reports from 1935 to 2022. *Int. journal legal medicine* **137**, 1535–1553 (2023).
- Amendt, J., Richards, C., Campobasso, C. P., Zehner, R. & Hall, M. J. Forensic entomology: applications and limitations. *Forensic Sci. Medicine, Pathol.* **7**, 379–392. <https://doi.org/10.1007/s12024-010-9209-2> (2011).
- Dawson, B. M., Ueland, M., Carter, D. O., McIntyre, D. & Barton, P. S. Bridging the gap between decomposition theory and forensic research on postmortem interval. *Int. journal legal medicine* **138**, 509–518 (2024).
- Henfße, C. & Madea, B. Estimation of the time since death in the early post-mortem period. *Forensic Sci. Int.* **144**, 167–175, <https://doi.org/10.1016/j.forsciint.2004.04.051> (2004). 100th Anniversary of the German Society of Legal Medicine.
- Vieira, R. B. et al. Biochemical analysis of vitreous humor and synovial fluid in the estimation of early postmortem interval: a meta-analytical approach. *J. forensic legal medicine* **108**, 102782–102782 (2024).
- Zilg, B., Bernard, S., Alkass, K., Berg, S. & Druid, H. A new model for the estimation of time of death from vitreous potassium levels corrected for age and temperature. *Forensic Sci. Int.* **254**, 158–166. <https://doi.org/10.1016/j.forsciint.2015.07.020> (2015).
- Zhou, C. & Byard, R. W. Factors and processes causing accelerated decomposition in human cadavers – an overview. *J. Forensic Leg. Medicine* **18**, 6–9. <https://doi.org/10.1016/j.jflm.2010.10.003> (2011).
- Hensge, C. & Madea, B. Estimation of the time since death. *Forensic Sci. Int.* **165**, 182–184, <https://doi.org/10.1016/j.forsciint.2007.05.017> (2007). Research in Forensic Medicine and Forensic Sciences: Basic Principles and Application in Practice.
- Cook, G. T. & MacKenzie, A. B. Radioactive isotope analyses of skeletal materials in forensic science: a review of uses and potential uses. *Forensic Sci. Medicine, Pathol.* **128**, 685–698. <https://doi.org/10.1007/s00414-014-0970-8> (2014).
- Swift, B. Dating human skeletal remains: Investigating the viability of measuring the equilibrium between 210po and 210pb as a means of estimating the post-mortem interval. *Forensic Sci. Int.* **98**, 119–126. [https://doi.org/10.1016/S0379-0738\(98\)00141-8](https://doi.org/10.1016/S0379-0738(98)00141-8) (1998).
- Swift, B., Lauder, I., Black, S. & Norris, J. An estimation of the post-mortem interval in human skeletal remains: a radionuclide and trace element approach. *Forensic Sci. Int.* **117**, 73–87, [https://doi.org/10.1016/S0379-0738\(00\)00451-5](https://doi.org/10.1016/S0379-0738(00)00451-5) (2001). Forensic Anthropology in the 21st Century.
- Alkass, K. et al. Age estimation in forensic sciences: Application of combined aspartic acid racemization and radiocarbon analysis*. *Mol. & Cell. Proteomics* **9**, 1022–1030. <https://doi.org/10.1074/mcp.M900525-MCP200> (2010).
- Alkass, K., Buchholz, B., Druid, H. & Spalding, K. Analysis of 14c and 13c in teeth provides precise birth dating and clues to geographical origin. *Forensic Sci. Int.* **209**, 34–41. <https://doi.org/10.1016/j.forsciint.2010.12.002> (2011).
- Pearson, D. D., Danforth, J. M. & Goodarzi, A. A. Radon (222rn) gas. In Wexler, P. (ed.) *Encyclopedia of Toxicology (Fourth Edition)*, 129–139, <https://doi.org/10.1016/B978-0-12-824315-2.00552-2> (Academic Press, Oxford, 2024), fourth edition edn.
- on the Effects of Atomic Radiation., U. N. S. C. *Sources and effects of ionizing radiation : United Nations Scientific Committee on the Effects of Atomic Radiation : UNSCEAR 2000 report to the General Assembly, with scientific annexes.* (United Nations, New York, 2000).

22. Danforth, J. M., Pearson, D. D. & Goodarzi, A. A. Ionizing radiation toxicology. In Wexler, P. (ed.) *Encyclopedia of Toxicology (Fourth Edition)*, 629–653, <https://doi.org/10.1016/B978-0-12-824315-2.00557-1> (Academic Press, Oxford, 2024), fourth edition edn.
23. Borak, T. B. & Baynes, S. A. Continuous measurements of outdoor ²²²Rn concentrations for three years at one location in Colorado. *Health Physics* **1958**(76), 418–420 (1999).
24. Oikawa, S. et al. A nationwide survey of outdoor radon concentration in Japan. *J. Environmental Radioactivity* **65**, 203–213 (2003).
25. Grasty, R. L. Summer outdoor radon variations in Canada and their relation to soil moisture. *Health Physics* **66**, 185–193. <https://doi.org/10.1097/00004032-199402000-00009> (1994).
26. Žunic, Z. et al. Radon survey in the high natural radiation region of Niška Banja, Serbia. *J. Environmental Radioactivity* **92**, 165–174 (2007).
27. Khan, S. M. et al. Rural communities experience higher radon exposure versus urban areas, potentially due to drilled groundwater well annuli acting as unintended radon gas migration conduits. *Sci. Reports* **14**, 3640–3640 (2024).
28. Cholowsky, N. L. et al. Consequences of changing Canadian activity patterns since the COVID-19 pandemic include increased residential radon gas exposure for younger people. *Sci. Reports* **13**, 5735–5735 (2023).
29. Irvine, J. L. et al. Social factors and behavioural reactions to radon test outcomes underlie differences in radiation exposure dose, independent of household radon level. *Sci. Reports* **12**, 15471–15471 (2022).
30. Khan, S. M. et al. Rising Canadian and falling Swedish radon gas exposure as a consequence of 20th to 21st century residential build practices. *Sci. Reports* **11**, 17551–17551 (2021).
31. Paquet, F. et al. ICRP Publication 137: Occupational intakes of radionuclides: Part 3. *Annals of the ICRP* **46**, 1–486 (2017).
32. Singh, P., Saini, K., Mishra, R., Sahoo, B. K. & Bajwa, B. S. Attached, unattached fraction of progeny concentrations and equilibrium factor for dose assessments from (222)Rn and (220)Rn. *Radiat. Environmental Biophysics* **55**, 401–410 (2016).
33. Osborne, R. V. Lead-210 and polonium-210 in human tissues. *Nat. (London)* **199**, 295–295 (1963).
34. Persson, B. R. & Holm, E. Polonium-210 and lead-210 in the terrestrial environment: a historical review. *J. Environmental Radioactivity* **102**, 420–429 (2011).
35. Leggett, R., Marsh, J., Gregoratto, D. & Blanchardon, E. A generic biokinetic model for noble gases with application to radon. *J. Radiol. Prot.* **33**, 413. <https://doi.org/10.1088/0952-4746/33/2/413> (2013).
36. Lim, S. M. et al. Indoor radon exposure increases tumor mutation burden in never-smoker patients with lung adenocarcinoma. *Lung Cancer* **131**, 139–146. <https://doi.org/10.1016/j.lungcan.2019.04.002> (2019).
37. Ziad, N., Zarki, R., Benmansour, M. B., Sayerh, T. & Laissaoui, A. Determination of ²¹⁰Pb in human skeletal remains from Morocco: implications for time since death assessment. *J. Radioanal. Nucl. Chem.* **292**, 315–319 (2012).
38. Arbova, D. L., Tolmachev, S. Y. & Brockman, J. D. A multi-collector ICP-MS method for quantification of plutonium, uranium, and americium in hair and nails of occupationally or medically exposed individuals. *Talanta (Oxford)* **270**, 125607–125607 (2024).
39. Simms, J. A. et al. Younger North Americans are exposed to more radon gas due to occupancy biases within the residential built environment. *Sci. Reports* **11**, 6724–10 (2021).
40. Ashrafkhani, B., Chambers, C., Wieser, M., Thompson, R. & Kwiatkowski, A. Optimizing ion optical design for laser ablation source in mass spectrometry. *J. Physics: Conf. Ser.* **2743**, <https://doi.org/10.1088/1742-6596/2743/1/012086> (2024).
41. Secco, L. et al. “omics” and postmortem interval estimation: A systematic review. *Int. Journal Molecular Sciences* **26**, 1034 (2025).
42. Bhojar, L., Mehar, P. & Chavali, K. Assessing the forensic implications of DNA degradation for PMI estimation using comet assay: A systematic review. *J. Forensic Legal Medicine* **109**, 102801–102801 (2025).
43. Cianci, V. et al. Potential role of mRNA in estimating postmortem interval: A systematic review. *Int. Journal Molecular Sciences* **25**, 8185 (2024).
44. Huang, W., Zhao, S., Liu, H., Pan, M. & Dong, H. The role of protein degradation in estimating postmortem interval and confirmation of cause of death in forensic pathology: A literature review. *Int. Journal Molecular Sciences* **25**, 1659 (2024).
45. Cláudia-Ferreira, A. et al. The future is now: Unraveling the expanding potential of human (necro)microbiome in forensic investigations. *Microorg. (Basel)* **11**, 2509 (2023).

Acknowledgements

M.E.W. and A.A.G. are each supported by NSERC Discovery Grants, and B.A. is supported by an NSERC SAP Grant. The work by the A.A.G. and M.E.W. teams is made possible by infrastructure funds from the Canada Foundation for Innovation, the Alberta Cancer Foundation, the Government of Alberta, and the Robson DNA Science Centre fund at the Arnie Charbonneau Cancer Institute.

Author contributions

F.T. conceived original idea. Current opportunity was realized by M.T. and A.A.G., and then further developed by all authors. B.A., M.T. and M.E.W. developed theoretical framework. B.A. and A.T. designed the model, and performed the numerical simulations. A.T. and B.A. carried out the programming implementation. B.A., M.E.W., and A.T. interpreted data and refined model. All authors provided critical feedback.

Declarations

Competing interests

The authors declare no competing interests.

Additional information

Correspondence and requests for materials should be addressed to B.A.

Reprints and permissions information is available at www.nature.com/reprints.

Publisher's note Springer Nature remains neutral with regard to jurisdictional claims in published maps and institutional affiliations.

Open Access This article is licensed under a Creative Commons Attribution-NonCommercial-NoDerivatives 4.0 International License, which permits any non-commercial use, sharing, distribution and reproduction in any medium or format, as long as you give appropriate credit to the original author(s) and the source, provide a link to the Creative Commons licence, and indicate if you modified the licensed material. You do not have permission under this licence to share adapted material derived from this article or parts of it. The images or other third party material in this article are included in the article's Creative Commons licence, unless indicated otherwise in a credit line to the material. If material is not included in the article's Creative Commons licence and your intended use is not permitted by statutory regulation or exceeds the permitted use, you will need to obtain permission directly from the copyright holder. To view a copy of this licence, visit <http://creativecommons.org/licenses/by-nc-nd/4.0/>.

© The Author(s) 2025